Laplace's Equation in Cartesian Coordinates and Satellite Altimetry

Variations in the gravitational potential and the gravitational force are caused by local variations in the mass distribution in the Earth. As described in an earlier lecture, we decompose the gravity field of the Earth into three fields:

- the main field due to the total mass of the earth;
- the second harmonic due to the flattening of the Earth by rotation; and
- anomalies which can be expanded in spherical harmonics or fourier series.

Here we are interested in anomalies due to local structure. Consider a patch on the Earth having a width and length less than about 1000 km or 1/40 of the circumference of the Earth. Within that patch we are interested in features as small as perhaps 1-km wavelength. Using a spherical harmonic representation would require 40,000 squared coefficients! To avoid this enormous computation and still achieve accurate results, we will treat the Earth as being locally flat. Here is a remove/restore approach that has worked well in our analysis of gravity and topography:

(1) Acquire a spherical harmonic model of the gravitational potential of the Earth and generate models of the relevant quantities (e.g., geoid height, gravity anomaly, deflection of the vertical, . . .) out to say harmonic 80. You may want to taper the harmonics between say 60 and 120 to avoid Gibb's phenomenon; this depends on the application.
(2) **Remove** that model from the local geoid, gravity, ... An alternate method is to remove a trend from the data and then apply some type of window prior to performing the fourier analysis. I do not recommend this practice because the trend being removed will contain a broad spectrum, it is dependent on the size of the area, and it cannot be restored accurately.
(3) Project the residual data onto a Mercator grid so the cells are approximately square and use the central latitude of the grid to establish the dimensions of the grid for Fourier analysis.
(4) Perform the desired calculation (e.g., upward continuation, gravity/topography transfer function, . . .).
(5) **Restore** the appropriate spherical harmonic quantity using the exact model that was removed originally.

Consider the disturbing potential

$$\Phi = U - U_o \qquad (1)$$

disturbing potential = total potential − reference potential

where, in this case, the reference potential comprises the reference Earth model plus the reference spherical harmonic model described in step (1) above. The disturbing potential satisfies Laplace's equation for an altitude, z, above the highest mountain in the area while it satisfies Poisson's equation below this level as shown in the following diagram.

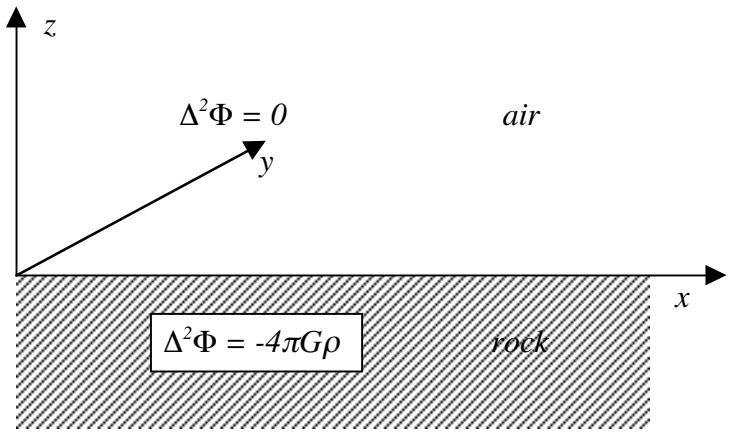

$\Phi(x,y,z)$ -- disturbing potential (total - reference)
G -- gravitational constant
ρ -- density anomaly (total - reference)

Laplace's equation is a second order partial differential equation in three dimensions.

$$\frac{\partial^2\Phi}{\partial x^2}+\frac{\partial^2\Phi}{\partial y^2}+\frac{\partial^2\Phi}{\partial z^2}=0, \qquad z>0 \tag{2}$$

Six boundary conditions are needed to develop a unique solution. Far from the region, the disturbing potential must go to zero; this accounts for 5 of the boundary conditions

$$\lim_{|x|\to\infty}\Phi=0, \quad \lim_{|y|\to\infty}\Phi=0, \quad \lim_{z\to\infty}\Phi=0 \tag{3}$$

At the surface of the earth (or at some elevation), one must either prescribe the potential or the vertical derivative of the potential.

$\Phi(x,y,0)=\Phi_o(x,y)$ -- Dirichlet

$$\frac{\partial\Phi}{\partial z}=-\Delta g(x,y) \qquad \text{-- Neumann} \tag{4}$$

To solve this differential equation, we'll use the 2-D fourier transform again where the forward and inverse transform are

$$F(\mathbf{k})=\int_{-\infty}^{\infty}\int_{-\infty}^{\infty} f(\mathbf{x})e^{-i2\pi(\mathbf{k}\cdot\mathbf{x})}d^2\mathbf{x} \tag{5}$$

$$f(\mathbf{x})=\int_{-\infty}^{\infty}\int_{-\infty}^{\infty} F(\mathbf{k})e^{i2\pi(\mathbf{k}\cdot\mathbf{x})}d^2\mathbf{k}$$

where $\mathbf{x} = (x, y)$ is the position vector, $\mathbf{k} = (1/\lambda_x, 1/\lambda_y)$ is the wavenumber vector, and $(\mathbf{k} \cdot \mathbf{x}) = k_x x + k_y y$. Fourier transformation reduces Laplace's equation and the surface boundary to

$$-4\pi^2\left(k_x^2 + k_y^2\right)\Phi(\mathbf{k},z) + \frac{\partial^2\Phi}{\partial z^2} = 0 \qquad (6)$$

$$\lim_{z\to\infty}\Phi(\mathbf{k},z) = 0, \qquad \Phi(\mathbf{k},0) = \Phi_o \qquad (7)$$

The general solution is

$$\Phi(\mathbf{k},z) = A(\mathbf{k})e^{2\pi|\mathbf{k}|z} + B(\mathbf{k})e^{-2\pi|\mathbf{k}|z} \qquad (8)$$

To satisfy the boundary condition as $z \to \infty$, the $A(\mathbf{k})$ term must be zero. To satisfy the boundary condition on the z=0 plane, $B(\mathbf{k})$ must be $\Phi(\mathbf{k},0)$. The final result is

$$\Phi(\mathbf{k},z) = \Phi_o(\mathbf{k},0)\, e^{-2\pi|\mathbf{k}|z} \qquad (9)$$

potential at altitude	=	potential at $z = 0$	×	upward continuation

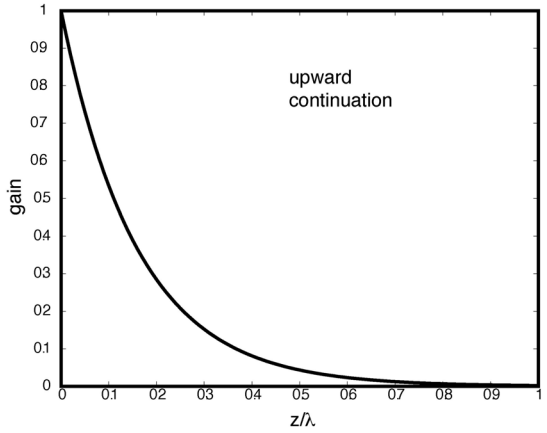

Figure 1. Gain of upward continuation kernel as a function of the altitude of the observation z, divided by the wavelength of the anomaly λ.

The upward continuation physics is the same for the potential and all of its derivatives. For example, if one measured gravity anomaly at the surface of the earth $\Delta g(\mathbf{x},0)$, then to compute the gravity at an altitude of z, one takes the fourier transform of the surface gravity, multiplies by the upward continuation kernel, and inverse transforms the result. This exponential decay of the signal with altitude is a fundamental barrier to recovery of small-scale gravity anomalies from a measurement made at altitude. Here are two important examples.

i) Marine gravity - Consider making marine gravity measurement on a ship which is 4 km above the topography of the ocean floor. (Most of the short-wavelength gravity anomalies are generated by the mass variations associated with the topography of the seafloor.) At a wavelength of say 8 km, the ocean surface anomaly will be attenuated by 0.043 from the amplitude of the seafloor anomaly.

ii) Satellite gravity - The typical altitude of an artificial satellite used to sense variations in the gravity field is 400 km so an anomaly having a 100-km wavelength will be attenuated by a factor of 10^{-11}! This is why radar altimetry (below), which measures the geoid height directly on the ocean surface topography is so valuable.

Derivatives of the gravitational potential

This solution to Laplace's equation can be used to construct all of the common derivatives of the potential. Suppose one has a complete survey over a patch on the surface of the earth so a fourier method can be used to convert among the different representations of the gravity field. This is particularly true for computing gravity anomaly from geoid height or deflection of the vertical. The general relation between the potential in the space domain (at any altitude) and the fourier transform of the surface potential is.

$$\Phi(\mathbf{x},z) = \int_{-\infty}^{\infty}\int_{-\infty}^{\infty} \Phi(\mathbf{k},\mathbf{0}) e^{-2\pi|\mathbf{k}|z} e^{i2\pi(\mathbf{k}\cdot\mathbf{x})} d^2\mathbf{k} \qquad (10)$$

The following table uses equation (10) and the definitions of the derivatives of the potential to construct the variety of anomalies. Before examining these relationships however, lets review some of the definitions in relation to what can be measured.

Gravitational potential	N - *geoid height* - Since the ocean surface is an equipotential surface, variations in gravitational potential will produce variations in the sea surface height. This can be measured by a radar altimeter.
First derivative of potential	Δg - *gravity anomaly* - This is the derivative of the potential with respect to z. It can be measured by an accelerometer such as a gravity meter. η, ξ - *deflection of the vertical* - These are the derivatives of the potential with respect to x and y, respectively. These are also

forces, however, they are usually measured by recording the tiny angle between a plumb bob and the vector pointing to the center of the earth. Over the ocean this is most easily measured by taking the along-track derivative of radar altimeter profiles.

Second derivative of potential- $\begin{bmatrix} \frac{\partial^2\Phi}{\partial x^2} & \frac{\partial^2\Phi}{\partial x\partial y} & \frac{\partial^2\Phi}{\partial x\partial z} \\ & \frac{\partial^2\Phi}{\partial y^2} & \frac{\partial^2\Phi}{\partial y\partial z} \\ & & \frac{\partial^2\Phi}{\partial z^2} \end{bmatrix}$ - *gravity gradient* - This is a symmetric tensor of second partial derivatives of the gravitational potential. A direct way of making this measurement is to construct a set of accelerometers each spaced at a distance of Δ in the x, y, and z directions. What is the minimum number of accelerometers needed to measure the full gravity gradient tensor? What can you say about the trace of this tensor when the measurements are made in free space? Below we'll develop an alternate method of measuring $\frac{\partial^2\Phi}{\partial z^2}$ over the ocean using a radar altimeter.

Table 1. Relationships among the various representations of the gravity field in free space.

	space domain	wavenumber domain
geoid height from the potential	$N(\mathbf{x}) \cong \frac{1}{g}\Phi(\mathbf{x},0)$	$N(\mathbf{k}) \cong \frac{1}{g}\Phi(\mathbf{k},0)$ (11)
gravity anomaly from the potential	$\Delta g(\mathbf{x},z) \cong -\frac{\partial\Phi}{\partial z}(\mathbf{x},z)$	$\Delta g(\mathbf{k},z) \cong 2\pi\lvert\mathbf{k}\rvert e^{-2\pi\lvert\mathbf{k}\rvert z}\Phi(\mathbf{k},0)$ (12)
deflection of the vertical from the potential (east slope and north slope)	$\eta(\mathbf{x}) = -\frac{\partial N}{\partial x} \cong -\frac{1}{g}\frac{\partial\Phi}{\partial x}$ $\xi(\mathbf{x}) = -\frac{\partial N}{\partial y} \cong -\frac{1}{g}\frac{\partial\Phi}{\partial y}$	$\eta(\mathbf{k}) \cong -\frac{i2\pi k_x}{g}\Phi(\mathbf{k},0)$ (13) $\xi(\mathbf{k}) \cong -\frac{i2\pi k_y}{g}\Phi(\mathbf{k},0)$
gravity anomaly from deflection of the vertical [*Haxby et al.,* 1983]		$\Delta g(\mathbf{k}) = \frac{ig}{\lvert\mathbf{k}\rvert}\left[k_x\eta(\mathbf{k}) + k_y\xi(\mathbf{k})\right]$ (14)
vertical gravity gradient from the curvature of the ocean surface	$\frac{\partial g}{\partial z} = g\left(\frac{\partial^2 N}{\partial x^2} + \frac{\partial^2 N}{\partial y^2}\right)$ (15)	

As an exercise, use Laplace's equation and the various definitions to develop gravity anomaly from vertical deflection (equation 14) and vertical gravity gradient from ocean surface curvature (equation 15).

Here is a practical example. Suppose one has measurements of geoid height $N(\mathbf{x})$over a large area on the surface of the ocean and we wish to calculate the gravity anomaly, $\Delta g(\mathbf{x},z)$ at altitude. The prescription is:

(1) remove an appropriate spherical harmonic model from the geoid;
(2) take the 2-D fourier transform of $\boldsymbol{N}(\mathbf{x})$;
(3) multiply by $g2\pi|\mathbf{k}|e^{-2\pi|\mathbf{k}|}$;
(4) take inverse 2-D fourier transform;
(5) restore the matching gravity anomaly calculated from the spherical harmonic model at altitude.

Conversion of geoid height to vertical deflection, gravity anomaly, and vertical gravity gradient from satellite altimeter profiles

As described above, geoid height $N(\mathrm{x})$ and other measurable quantities such as gravity anomaly $g(\mathrm{x})$ are related to the anomalous gravitational potential $\Phi(\mathrm{x},z)$ through Laplace's equation. It is instructive to go through an example of how measurements of ocean surface topography from satellite altimetry can be used to construct geoid height, deflection of the vertical, gravity anomaly, and vertical gravity gradient.

The surface of the ocean is displaced both above and below the reference ellipsoidal shape of the Earth (Figure 2). These differences in height arise from variations in gravitational potential (i.e., geoid height) and oceanographic effects (tides, large-scale currents, el Nino, eddies, . . .). Fortunately, the oceanographic effects are small compared with the permanent gravitational effects so a radar altimeter can be used to measure these bumps and dips. At wavelengths less than about 200 km, bumps an dips in the ocean surface topography reflect the topography of the ocean floor and can be used to estimate seafloor topography in areas of sparse ship coverage.

Radar altimeters are used to measure the height of the ocean surface above the reference ellipsoid (i.e., the satellite above the ellipsoid H^* minus the altitude above the ocean surface H). A GPS, or ground-based tracking system, is used to establish the position of the radar H^* (as a function of time) to an accuracy of better than 0.1 m. The radar emits 1000 pulses per second at Ku-band. These spherical wave fronts reflect from the closest ocean surface (nadir) and return to the satellite where the two-way travel times is recorded to an accuracy of 3 nanoseconds (1-m range variations mostly due to ocean waves). Averaging thousands of pulses reduces the noise to about 30 mm. If one is interested in making an accurate geoid height map such, as shown in Figure 4, then many sources of error must be considered and somehow removed. However, if the final product of interest is one of the derivatives of the potential then it is best to take the

along-track derivative of each profile to develop along-track sea surface slope. In this case, the point-to-point precision of the measurements is the limiting factor.

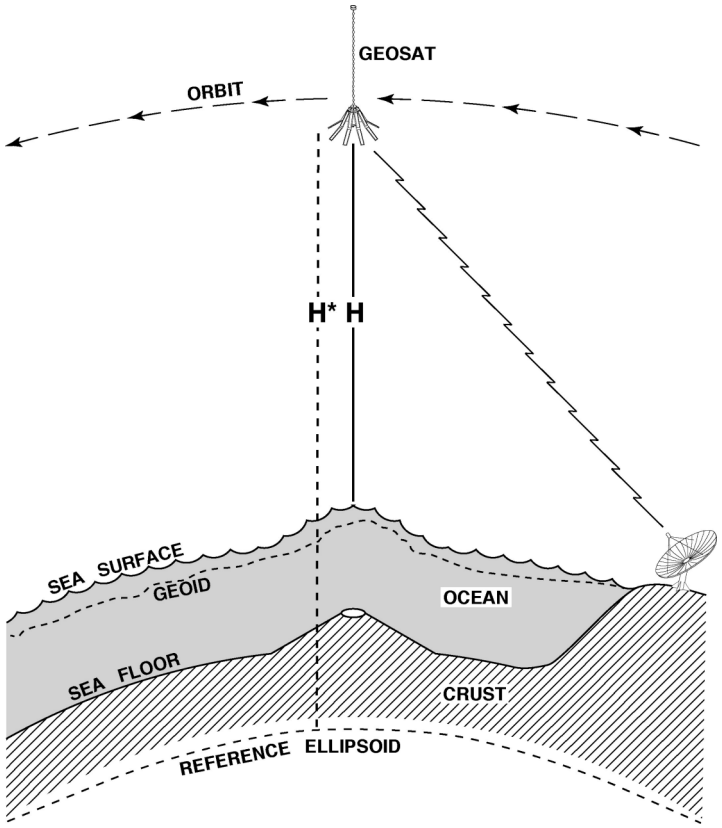

Figure 2. Schematic diagram of a radar altimeter orbiting the earth at an altitude of 800 km.

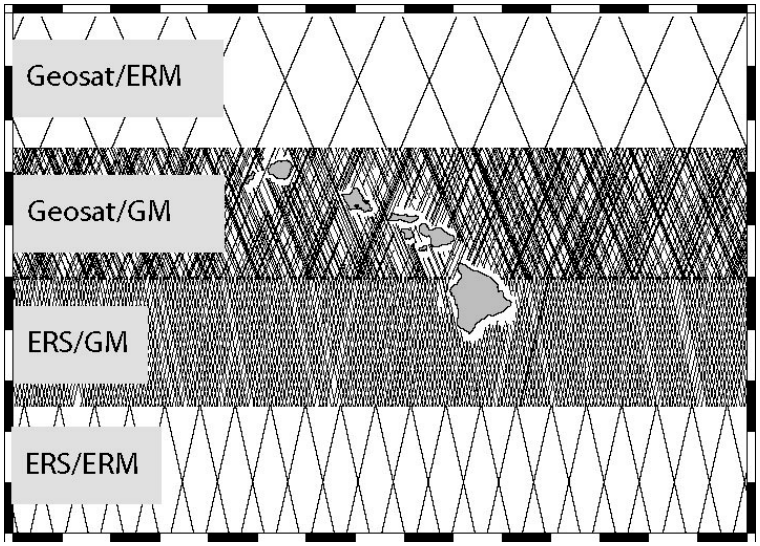

Figure 3. Ground tracks for two radar altimeters that have provided adequate coverage of the ocean surface. This is a 1500-km by 1000-km area around Hawaii. Geosat/ERM (US Navy) is the exact repeat orbit phase of the Geosat altimeter mission (US Navy, 1985-89). These ground tracks repeat every 17 days to monitor small changes in ocean surface height caused by time-varying oceanographic effects. Geosat/GM ground tracks were acquired during a 1.5-year period when the orbit was allowed to drift. Similarly ERS/GM was a European Space Agency phase of the ERS mission that acquired non-repeat profiles for 1 year. ERS/ERM is the 35-day repeat phase of the ERS mission.

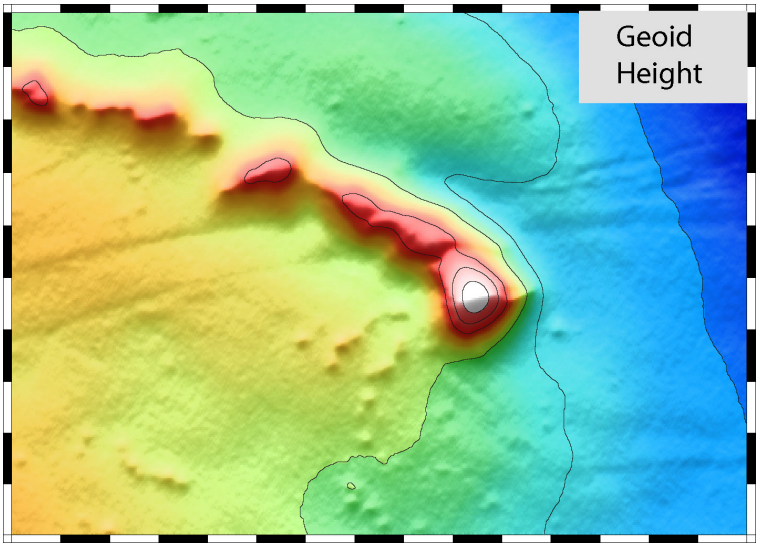

Figure 4. Geoid height above the WGS84 ellipsoid in meters (5-m contour interval) derived from altimeter profiles in Figure 3. The geoid height is dominated by long-wavelengths so it is difficult to observe the small-scale features caused by ocean-floor topography. These can be enhanced by computing either the horizontal derivative (ocean surface slope) or the vertical derivative (gravity anomaly).

To avoid a crossover adjustment of the data, ascending and descending satellite altimeter profiles are first differentiated in the along-track direction resulting in geoid slopes or along-track vertical deflections. These along-track slopes are then combined to produce east η and north ξ components of vertical deflection [*Sandwell,* 1984]. Finally the east and north vertical deflections are used to compute both gravity anomaly and vertical gravity gradient. The algorithm used for gridding the altimeter profiles is an iteration scheme that relies on rapid transformation from ascending/descending geoid slopes to north/east vertical deflection and vice versa. The details for converting along-track slope into east and north components of deflection of the vertical are provided in the Appendix and also in a reference [*Sandwell and Smith,* 1997]. You probably don't need to know these details unless you plan to do research in marine gravity.

Figure 5. East component of sea surface slope $\eta(\mathbf{x})$ derived from Geosat and ERS altimeter profiles. Note this component is rather noisy because the altimeter tracks (Figure 3) run mainly in a N-S direction.

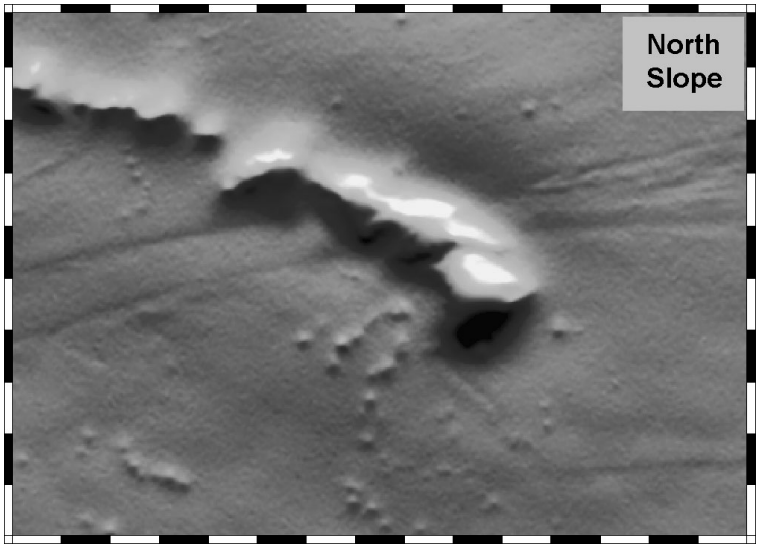

Figure 6. North component of sea surface slope $\xi(\mathbf{x})$ derived from Geosat and ERS altimeter profiles. Note this component has lower noise because the altimeter tracks (Figure 3) run mainly in a N-S direction.

To compute gravity anomaly (Figure 7) from a dense network of satellite altimeter profiles of geoid height (Figure 2), one constructs grids of east η and north ξ vertical deflection (Figures 5 and 6). The grids are then Fourier transformed and Eq. (5) is used to compute gravity anomaly. At this point one can add the long wavelength gravity field from the spherical harmonic model to

the gridded gravity values in order to recover the total field; the resulting sum may be compared with gravity measurements made on board ships. A more complete description of gravity field recovery from satellite altimetry can be found in [*Hwang and Parsons*, 1996; *Sandwell and Smith*, 1997; *Rapp and Yi*, 1997].

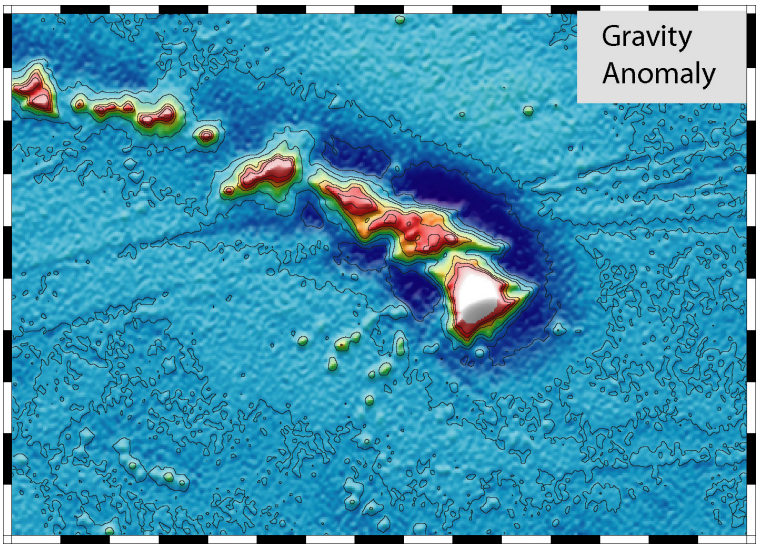

Figure 7. Gravity anomaly $\Delta g(\mathbf{x})$ derived from east and north components of sea surface slope using equation (14). (50 mGal contour interval)

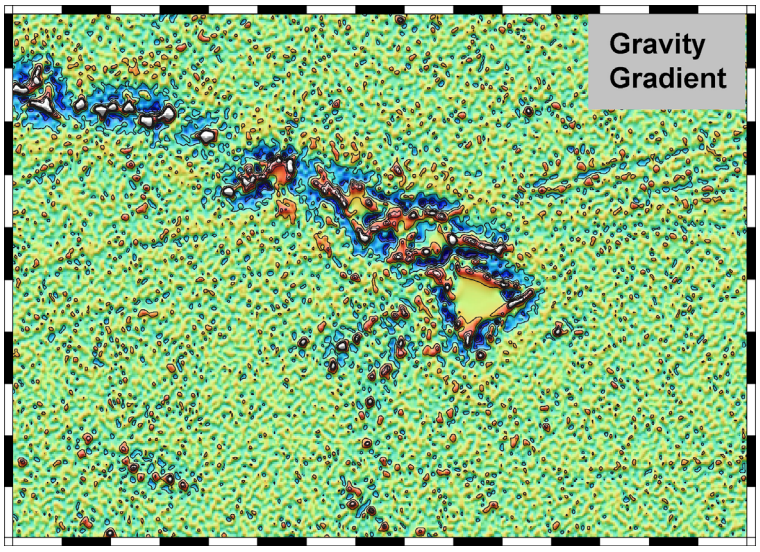

Figure 8. Vertical gravity gradient $dg(\mathbf{x})/\delta z$ derived from east and north components of sea surface slope using equation (15). Note this second derivative of the geoid amplifies the shortest wavelengths; compare with the original geoid (Figure 3). Noise in the altimeter measurements has been amplified resulting in an artificial texture. (100 Eotvos contour interval)

There is an important issue for constructing gravity anomaly from sea surface slope that is revealed by a simplified version of equation (14). Consider the sea surface slope and gravity anomaly across a two-dimensional structure which depends on *x* but not *y*. The *y*-component of slope is zero so conversion from sea surface slope to gravity anomaly is simply a Hilbert transform:

$$\Delta g(k_x) = ig\,\mathrm{sgn}(k_x)\eta(k_x) \tag{16}$$

Now it is clear that one μrad of sea surface slope maps into 0.98 mGal of gravity anomaly and similarly one μrad of slope error will map into ~1 mGal of gravity anomaly error. Thus the accuracy of the gravity field recovery is controlled by the accuracy of the sea surface slope measurement.

APPENDIX - *Vertical Deflections from Along-Track Slopes*

Consider for the moment the intersection point of an ascending and a descending satellite altimeter profile. The derivative of the geoid height *N* with respect to time *t* along the ascending profile is

$$\dot{N}_a \equiv \frac{\partial N_a}{\partial t} = \frac{\partial N}{\partial \theta}\,\dot{\theta}_a + \frac{\partial N}{\partial \phi}\,\dot{\phi}_a \tag{B1}$$

and along the descending profile is

$$\dot{N}_d = \frac{\partial N}{\partial \theta}\,\dot{\theta}_d + \frac{\partial N}{\partial \phi}\,\dot{\phi}_d \tag{B2}$$

where is θ geodetic latitude and ϕ is longitude. The functions θ and ϕ are the latitudinal and longitudinal components of the satellite ground track velocity. It is assumed that the satellite altimeter has a nearly circular orbit so that its velocity depends mainly on latitude; at the crossover point the following relationships are accurate to better than 0.1%.

$$\dot{\theta}_a = -\dot{\theta}_d \qquad \phi_a = \phi_d \tag{B3}$$

The geoid gradient (deflection of the vertical) is obtained by solving (B1) and (B2) using (B3).

$$\frac{\partial N}{\partial \phi} = \frac{1}{2\dot{\phi}} \left(\dot{N}_a + \dot{N}_d\right) \tag{B4}$$

$$\frac{\partial N}{\partial \theta} = \frac{1}{2|\dot{\theta}|} \left(\dot{N}_a - \dot{N}_d\right) \tag{B5}$$

It is evident from this formulation that there are latitudes where either the east or north component of geoid slope may be poorly determined. For example, at ±72˚ latitude, the Seasat and Geosat altimeters reach their turning points where the latitudinal velocity θ goes to zero and thus (B4) becomes singular. In the absence of noise this is not a problem because the ascending and descending profiles are nearly parallel so that their difference goes to zero at the same rate that the latitudinal velocity goes to zero. Of course in practice altimeter profiles contain noise, so that the north component of geoid slope will have a signal to noise ratio that decreases near ±72˚ latitude. Similarly for an altimeter in a near polar orbit, the ascending and descending profiles are nearly anti-parallel at the low latitudes; the east component of geoid slope is poorly determined and the north component is well determined. The optimal situation occurs when the tracks are nearly perpendicular so that the east and north components of geoid slope have the same signal to noise ratio.

When two or more satellites with different orbital inclinations are available, the situation is slightly more complex but also more stable. Consider the intersection of 4 passes as shown in the following diagram.

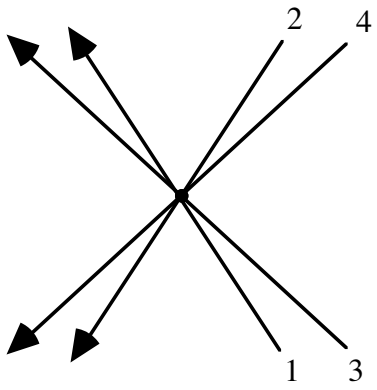

The along-track derivative of each pass can be computed from the geoid gradient at the crossover point

$$\begin{bmatrix} \dot{N}_1 \\ \dot{N}_2 \\ \dot{N}_3 \\ \dot{N}_4 \end{bmatrix} = \begin{bmatrix} \dot{\theta}_1 & \dot{\phi}_1 \\ \dot{\theta}_2 & \dot{\phi}_2 \\ \dot{\theta}_3 & \dot{\phi}_3 \\ \dot{\theta}_4 & \dot{\phi}_4 \end{bmatrix} \begin{bmatrix} \frac{\partial N}{\partial \theta} \\ \frac{\partial N}{\partial \phi} \end{bmatrix} \tag{B6}$$

or in matrix notation

$$\dot{\mathbf{N}} = \boldsymbol{\Theta} \quad \nabla N \tag{B7}$$

Since this is an overdetermined system, the 4 along-track slope measurements cannot be matched exactly unless the measurements are error-free. In addition, an a-priori estimate of the error in the along-track slope σ_i measurements can be used to weight each equation in (B6) (i.e. divide each of the four equations by σ_i). The least squares solution to (B7) is

$$\nabla N = \left(\boldsymbol{\Theta}^t \boldsymbol{\Theta}\right)^{-1} \boldsymbol{\Theta}^t \dot{\mathbf{N}} \tag{B8}$$

where t and -1 are the transpose and inverse operations, respectively. In this case a 2 by 4 system must be solved at each crossover point although the method is easily extended to three or more satellites. Later we will assume that every grid cell corresponds to a crossover point of all the satellites considered so this small system must be solved many times.

In addition to the estimates of geoid gradient, the covariances of these estimates are also obtained

$$\begin{bmatrix} \sigma^2_{\theta\theta} & \sigma^2_{\theta\phi} \\ \sigma^2_{\phi\theta} & \sigma^2_{\phi\phi} \end{bmatrix} = (\boldsymbol{\Theta}^t \boldsymbol{\Theta})^{-1} \tag{B9}$$

Since Geosat and ERS-1 are high inclination satellites, the estimated uncertainty of the east component is about 3 times greater than the estimated uncertainty of the north component at the equator. At higher latitudes of 60˚-70˚ where the tracks are nearly perpendicular, the north and east components are equally well determined. At 72˚ north where the Geosat tracks run in a westerly direction, the uncertainty of the east component is low and the higher inclination ERS-1 tracks prevent the estimate of the north component from becoming singular at 72˚.

Finally, the east η and north ξ components of vertical deflection are related to the two geoid slopes by

$$\eta = -\frac{1}{a \cos\theta}\frac{\partial N}{\partial \phi} \qquad \text{(B10)}$$

$$\xi = -\frac{1}{a}\frac{\partial N}{\partial \theta} \qquad \text{(B11)}$$

where a is the mean radius of the earth.

REFERENCES

Haxby, W. F., Karner, G. D., LaBrecque, J. L., and Weissel, J. K. (1983). Digital images of combined oceanic and continental data sets and their use in tectonic studies. *EOS Trans. Amer. Geophys. Un.* **64**, 995-1004.

Hwang, C., and Parsons, B. (1996). An optimal procedure for deriving marine gravity from multi-satellite altimetry. *J. Geophys. Int.* 125, 705-719.

Rapp, R. H., and Yi, Y. (1997). Role of ocean variability and dynamic topography in the recovery of the mean sea surface and gravity anomalies from satellite altimeter data. *J. Geodesy* **71**, 617-629.

Sandwell, D. T. (1984). A detailed view of the South Pacific from satellite altimetry. *J. Geophys. Res.* **89**, 1089-1104.

Sandwell, D. T., and Smith, W. H. F. (1997). Marine gravity anomaly from Geosat and ERS-1 satellite altimetry. *J. Geophys. Res.* **102**, 10,039-10,054.

Yale, M. M., D. T. Sandwell, and W. H. F. Smith, Comparison of along-track resolution of stacked Geosat, ERS-1 and TOPEX satellite altimeters, *J. Geophys. Res., 100,* p. 15117-15127, 1995.